New method to predict truck-semitrailer jackknifing effect

Roberto Spinola Barbosa

Polytechnic School of University of Sao Paulo,
Av. Prof. Mello Moraes,
2231, cep. 05508-970,
Sao Paulo, SP, Brazil
Email: spinola@usp.br

Abstract: A new method based on two articulated bodies with internal inertial force, similar to the structural buckling effect, is proposed to describe the unstable yaw relative angular movement between truck and semitrailer, known as jackknifing. An analytic expression is derived from the proposed linear model, allowing the prediction of the deceleration limit prior to the yaw instability phenomenon. A detailed non-linear model with 19 degrees of freedom was developed and used as a simulations tool to verify dynamic performance. The analytical results of the jackknife effect were validated by comparison with the instability tendency simulated with a complete vehicle dynamic model. The results show good agreement between the proposed analytical expression and the numerical simulation. The proposed analytic expression is independent of the vehicle speed and does not require a stability analysis or an integration process, unlike all other techniques available in the literature.

Keywords: jackknifing; truck; dynamic; safety; instability.

Reference to this paper should be made as follows: Barbosa, R.S. (2020) 'New method to predict truck-semitrailer jackknifing effect', *Int. J. Heavy Vehicle Systems*, Vol. 27, No. 6, pp.840–860.

Biographical notes: Roberto Spinola Barbosa is currently a PhD. He is an Associated Professor at Mechanical Engineering Department at the Polytechnic School of the University of Sao Paulo. He received his PhD. in University of Sao Paulo, Brasil, in 1999. His interests and research area includes multibody systems and vehicle system dynamic modelling, simulation, control and safety.

1 Introduction

Jackknifing is a yaw instability of a truck, which causes the trailer to rotate, relative to the tractor (see Figure 1). As a consequence, the driver loses the vehicle control and the trailer can extend to adjacent lanes causing partial or complete traffic obstruction, collision with oncoming traffic or parked vehicles, causing accidents and injuries, with potential of being catastrophic due to the size and weight of the vehicles involved. The jackknifing phenomenon is known to happen at high speeds or under emergency braking,

when the wheels are locked and the vehicle tends to swing around. If the truck travels fast and the driver needs to brake suddenly then the entire truck, along with the trailers, can get into a skid situation. If the tractor and trailer skid long enough, the trailer will be, most certainly, jack-knifed, with the rig finally coming to a stop.

Figure 1 Truck/semitrailer jackknifing (Art from AS in internet) (see online version for colours)

These phenomena can also be aggravated in poor surface adherence conditions (due to contaminations by dust, oil, leaves, irregularities, water, ice, etc.) when a slippery road causes the reduction or even loss of wheel driving contact forces capabilities. The brake distribution between truck and trailer is another relevant aspect. The brake system is designed to sustain the adequate brake distribution. Jackknifing usually occurs with empty trailers or when the weight of the load is badly distributed. The tractor and the trailer brakes are usually designed for a full load, and are far too powerful for an underweight trailer. When severe braking is applied, the wheels could lock up, causing skidding, and harming the drivability. Another possibility is the trailer brake failure or malfunction due to pneumatic connections problems.

Additionally downshifting or engine retardants can also decelerate the set asymmetrically. Particularly, when entering in a curve too quickly for the truck driver to handle, equipment malfunction can also increase the risk of jackknifing. The driver inability, or when in a dangerous operational speed, incompatible with the road geometry, can worsen the risks and should be avoided.

To prevent such risks, it is imperative to understand the instability phenomenon and to find a representative expression containing the main contributing factors, quantifying each participation, in order to be able to handle them to minimise potential risks. Pointing out which manoeuvres should be avoided, should also contribute to better driving practices to haul trucks and trailer sets.

In the literature review, it has been found that most of the public available works relies on the analysis of the stability of the vehicle's dynamic model. The first studies on the jackknifing effect began in the 1960s (Talbott, 1962). Since then, several authors have

revisited the subject. The stability of car-trailer using planar model, particularly the yaw instability, has been intensively investigated by several authors such as Genta (2006), Pacejka (2006), Luijten (2010), Masory and Grainer (2004), Ding et al. (2014) and has been widely publicised in the literature.

The articulated vehicles stability is generally evaluated using the differential equations of the system model (Genta, 2006; Pacejka, 2006; Luijten, 2010). The handling of the linearised model that describes small changes in the lateral and yaw dynamics of these vehicles has been employed. All roots (λ) of the characteristic polynomial equation of the linear dynamic system should have negative real parts for the system to be stable (*Routh-Hurwitz* criterion). *Luijten* states that the vehicle combination experiences a saddle-node bifurcation, and that the fourth critical speed determines a monotonic stability. The third *Hurwitz* determinant determines the *hopf* bifurcation and concludes that, in practice, many vehicles with one articulation are stable (Genta, 2006; Luijten, 2010).

Analyses, such as yaw or lateral instability, bifurcation, *hopf* bifurcation or centre manifold theory on a non-linear model, have been used to describe the vehicle unstable behaviour. Ding et al. (2014) uses a planar linearised simple model to study the bifurcation that is sufficient to capture deleterious and dangerous unstable behaviour.

For an oversteered truck (Wideberg and Dahlberg, 2013), once a steering command (δ_1) is given, the vehicle is stable at low velocities. However, it will become unstable if the vehicle speed is beyond a certain limit known as the critical speed (Pacejka, 2006; Luijten, 2010; Ding et al., 2014; Costa Neto, 2016). The yaw velocity gain of an understeered single vehicle (the yaw rate r_1 over δ_1 as presented in the right graph of Figure 2) reaches its maximum at the characteristic speed. Hence, an understeered vehicle is directionally stable at any speed. The yaw velocity gain of a neutrally steered vehicle increases linearly with speed. Finally, the yaw velocity gain of an oversteered vehicle goes to infinity at the critical speed, as it is unstable beyond this velocity, as shown in Figure 2.

Figure 2 Steady-state cornering characteristics for a single vehicle (from *luijten*): (a) handling diagram and (b) yaw gain diagram

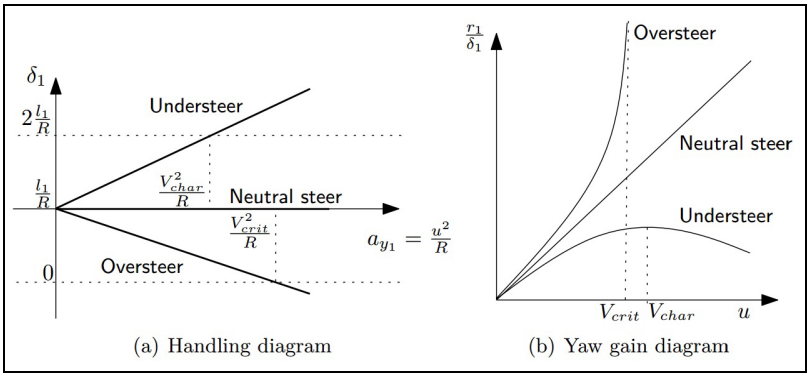

The jackknifing effect on the straight road section was recreated by the simulation of a complete model considering brake deceleration (Pinxteren, 2010). Also Kaneko et al. (2002) have modelled the jackknifing effect by adopting a longitudinal road inclination and a gradient on the lateral direction. Several experimental measurements with

instrumented vehicles have been performed (Dunn and Hoover, 2004; Ashley et al., 2014; Li et al., 2016; Bouteldja and Cerezo, 2011; Elhemly et al., 2013). Several studies in control technique are also developed (Yuan and Zhu, 2016). Although jackknifing phenomenon has been deeply analysed, few contributions to the design or practical operational recommendations to the driver have been published.

The stability of guided vehicles is usually associated with the tyre contact force, which is a function of the wheel's contact slip. The model describing this behaviour is addressed considering the ratio between the tyre path slip-speed divided by the vehicle speed. Therefore, the model will have a damping matrix associated with the velocities' states divided by the modulus of the vehicle speed. In this case, the modal damping factor is inversely proportional to the speed (Barbosa and Costa Neto, 1996), which can be lower than or equal to zero for large speeds, then destabilising the systems. The result from this type of approach is always associated to a speed limit.

The motivation of this research is to further the investigation associated with the vehicle yaw movement, subjected to an inertial compressive inter-body force, and the reactive torque produced by the lateral force of the truck's tyres, that can sustain it. Therefore, the main focus of this research is to investigate the dynamic performance of the vehicle's handling and its stability.

2 New proposition

The proposition of this new method is that the yaw instability phenomenon (jackknifing) occurs mainly due to eventual tractor/trailer internal compressive force, produced by deceleration under non-balanced retarding force distribution. To this end, the column-buckling model is employed to characterise a two-body folding movement under compressive load, to be described next.

2.1 Buckling model

The traditional elastic continuous beam buckling (Figure 3(A)) is characterised by a sudden sideways instability of a structural member subjected to high compressive P load. This load can be calculated with the elastic line equation (*Timoshenko*), to obtain the critical load P_{CR}, prior to buckling, as:

$$P = P_{CR} = \frac{\pi E I}{L^2} \tag{1}$$

Also, the critical load for a bi-articulated rigid bar system is shown in Figure 3(B), which can be solved in a similar fashion, by equating the moment of the compressive force P to the internal restitutive torque of the elastic angular spring k_{φ}, to get the critical load P_{CR} as:

$P L \sin\phi = k_{\phi}(2\phi)$, which for small φ reduces to $\left(P L - 2k_{\phi}\right)\phi = 0$,

$$\text{and } P_{CR} = \frac{2k_{\phi}}{L} \tag{2}$$

showing that the second possible unstable solution is for $\phi = 0$ (beams aligned).

Figure 3 Buckling models

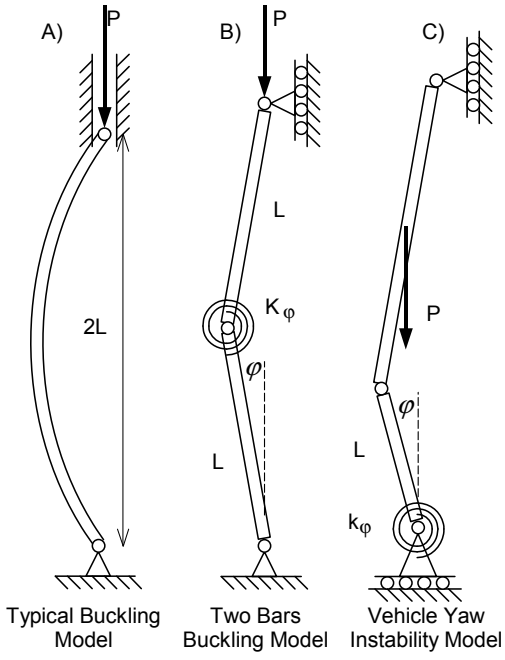

3 Proposed analytical expression

The analytical expression proposed in this research to describe/study the jackknifing effect is based on the beam-buckling equilibrium phenomena as presented earlier. To obtain a static solution of the yaw stability limits for the vehicle, an analytical inertial linear model, based on the beam-buckling model, as presented in Figure 3(C), has been idealised. In this approach, the yaw (*buckling*) movement will only happen if the inertial reaction load P from the trailer, due to an eventual non-balanced distribution of retarding forces, is greater than the restoring torque produced by the tyre lateral contact forces (represented by stiffness k_φ). This proposed model does not depend on the vehicle speed and can determine the maximum deceleration stability limits.

When the brake force F_{brake} is eventually more intense on the tractor than on the trailer, the trailer tends to push it, producing the force P applied on the fifth wheel of the tractor by the kingpin of the trailer (*KP* shown in Figure 4). When the set is aligned in a straight trajectory, an unstable equilibrium position is established. However, any perturbation or deviation will produce a yaw movement (jackknifing), when the torque of the load P is greater than the restoring torque produced by the tyre lateral forces of the tractor wheels (F_{yi} in Figure 4).

The translational dynamic equilibrium equation of the tractor with mass m_1 on the *D'Alembert's* form is expressed as:

$$(\vec{P} + \vec{F}_{\text{brake}} - m_1 \vec{a}_G) = 0 \tag{3}$$

which shows that the kingpin force P, due to eventual non-proportional braking forces between tractor ($F_{brake}= -F_{x1} - F_{x2}$) and trailer ($F_{x3}$), acts as a compressive force during deceleration.

Figure 4 Tractor force distribution

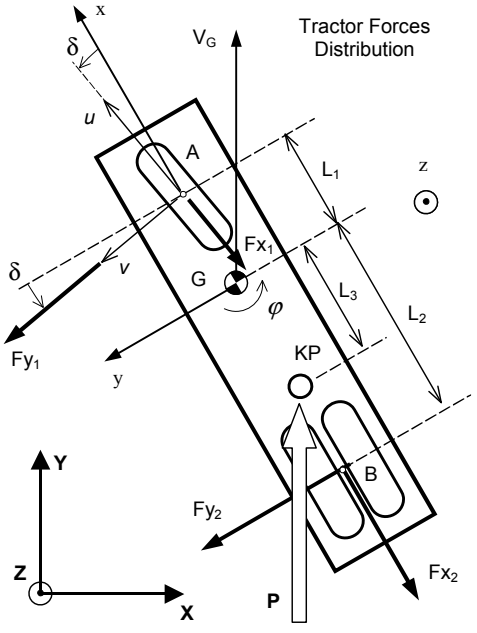

Applying the angular *Euler's* equation for a planar bicycle simplified model according to Figure 4, and expressing the angular momentum of the tractor in the moving local reference frame (*Gxyz*), fixed on the tractor, and for a pole coincident with its centre of mass G, gives:

$$[I]_G[\dot{\omega}]+[\omega]^T \wedge [I]_G[\omega] = M_G \tag{4}$$

where $[I]_G$ is the tractor inertia matrix, $[\omega]$ is the angular speed vector, $[\dot{\omega}]$ is the angular acceleration vector and M_G is the moment of the external forces, all related to the pole G. The free body force diagram presented in Figure 4, for a symmetric vehicle to the longitudinal axis, shows that the planar dynamic angular equation, will lead to the rotational equation in the z direction only as:

$$J_{Gz}\alpha_z = PL_3 \sin\phi + F_{y1}L_1 \cos\delta - F_{y2}L_2 - F_{x1}L_1 \sin\delta \tag{5}$$

where δ is the front wheel steer angle, P is the kingpin force, and φ is the tractor yaw angle. Considering a null steering angle δ, the previous expression reduces to:

$$J_{Gz}\alpha_z = PL_3 \sin\phi + F_{y1}L_1 - F_{y2}L_2 \tag{6}$$

clearly showing the '*battle*' between the aligning torques of the wheels lateral forces (F_{yi}) against the kingpin force P moment. Note that, in the simple bicycle model with no

steering angle ($\delta = 0$), the longitudinal component of the brake force F_{xi} does not contribute to the right side of the angular equation.

The lateral tyre force F_{iy} (for the ith tyre) is usually described as proportional to the side-slip of the tyre contact path ξ_{iy}:

$$F_{iy} = -C_{iy}\,\xi_{iy}\text{, where } \xi_{iy} = \frac{V_{iv}}{|\vec{V}|} \tag{7}$$

Therefore, the side-slip of each tyre should be determined. The velocity at contact point A of the front wheel (see Figure 4) is obtained from the velocity field equation. Taking the absolute velocity of the tractor's centre of mass $\vec{V}_G = \dot{X}_G\vec{i} + \dot{Y}_G\vec{j}$, written in the planar moving reference frame *Gxyz,* with the unit versors $\vec{i}\ \vec{j}\ \vec{k}$, it is possible to obtain the velocity of the front wheel contact point A as:

$$\vec{V}_A = \vec{V}_G + \vec{\omega} \wedge (A-G) = \left(\dot{X}_G\vec{i} + \dot{Y}_G\vec{j}\right) + \dot{\phi}\vec{k} \wedge L_1\vec{i} = \dot{X}_G\vec{i} + \left(\dot{Y}_G + L_1\dot{\phi}\right)\vec{j} \tag{8}$$

Projecting the velocity of point A on the reference frame $A\,\vec{u}\,\vec{v}$, aligned with the front wheel, rotated by the steering angle δ, the following expressions are obtained for the velocity of the front wheel contact point A:

$$\vec{V}_A = \dot{X}_G\vec{i} + \left(\dot{Y}_G + L_1\dot{\phi}\right)\vec{j} = \dot{X}_G\left(\cos\delta\,\vec{u} - \sin\delta\,\vec{v}\right) + \left(\dot{Y}_G + L_1\dot{\phi}\right)\left(\sin\delta\,\vec{u} + \cos\delta\,\vec{v}\right) \tag{9}$$

$$\vec{V}_A = \left[\dot{X}_G\cos\delta + \left(\dot{Y}_G + L_1\dot{\phi}\right)\sin\delta\right]\vec{u} + \left[-\dot{X}_G\sin\delta + \left(\dot{Y}_G + L_1\dot{\phi}\right)\cos\delta\right]\vec{v} \tag{10}$$

By considering a small steering angle ($\cos\delta = 1$ and $\sin\delta = \delta$), gives the following expression for the front wheel lateral direction velocity ($V_{Av} = \vec{V}_A \cdot \vec{v}$):

$$\vec{V}_A = \left[\dot{X}_G + \left(\dot{Y}_G + L_1\dot{\phi}\right)\delta\right]\vec{u} + \left[-\dot{X}_G\,\delta + \left(\dot{Y}_G + L_1\dot{\phi}\right)\right]\vec{v} \;\rightarrow\; V_{Av} = -\delta\,\dot{X}_G + \left(\dot{Y}_G + L_1\dot{\phi}\right) \tag{11}$$

Therefore, the front wheel lateral force at point A F_{Av} (see Figure 4) will be proportional to the corner stiffness (C_{Ay}) of the front tyre as described in equation (7):

$$F_{Av} = -C_{Ay}\left(\frac{-\delta\,\dot{X}_G + \left(\dot{Y}_G + L_1\dot{\phi}\right)}{|V_x|}\right) = -C_{Ay}\left(-\delta + \frac{\left(\dot{Y}_G + L_1\dot{\phi}\right)}{\dot{X}_G}\right) \tag{12}$$

where $V_x \cong \dot{X}_G$. In a similarly fashion, the lateral force for the rear wheel B will be given by:

$$F_{Bv} = -C_{By}\left(\frac{-\delta\,\dot{X}_G + \left(\dot{Y}_G - L_2\dot{\phi}\right)}{|V_x|}\right) = -C_{By}\left(-\delta + \frac{\left(\dot{Y}_G - L_2\dot{\phi}\right)}{\dot{X}_G}\right) \tag{13}$$

By considering that prior to the instability both vehicles are in a rectilinear trajectory with $\delta = 0$ and $\dot{\phi} = 0$, gives the force for the front and rear wheels as:

$$F_{Ay} = -C_{Ay}\frac{\dot{Y}_G}{\dot{X}_G}, \text{ for the front wheel, and } F_{By} = -C_{By}\frac{\dot{Y}_G}{\dot{X}_G}, \text{ for the rear wheel} \quad (14)$$

The components of the vehicle's absolute speed $\vec{V}_G$ can be expressed in the auxiliary reference frame as:

$$\dot{X}_G = |\vec{V}_G|\cos\phi;\ \dot{Y}_G = -|\vec{V}_G|\sin\phi \rightarrow \frac{\dot{Y}_G}{\dot{X}_G} = -\tan\phi \quad (15)$$

Finally, using the previous relation, the lateral tyre forces will be functions of the corner stiffness of each tyre and angle φ:

$$F_{Ay} = C_{Ay}\tan\phi \text{ and } F_{By} = C_{By}\tan\phi \quad (16)$$

Applying these results into the moment equation, and considering a steady state aligned unstable equilibrium ($\varphi \approx 0$; $\alpha_z = 0$), gives:

$$J_{Gz}\alpha_z = PL_3\sin\phi + C_{y1}L_1\tan\phi - C_{y2}L_2\tan\phi, \text{ and } \left(PL_3 + C_{y1}L_1 - C_{y2}L_2\right)\phi = 0 \quad (17)$$

The solutions of these equations for $\varphi = 0$ (vehicles aligned), gives the critical load P_{critic} beyond which the yaw instability occurs (jackknifing) as:

$$P_{critic} = \frac{C_{y2}L_2 - C_{y1}L_1}{L_3} \quad (18)$$

From the dynamic equilibrium equation for the tractor (with mass m_1) and for the trailer (with mass m_2) in the longitudinal direction with braking forces F_{xi}, give, respectively:

$$P - F_{x1} - F_{x2} - m_1\ddot{X}_{G1} = 0 \text{ and } -P - F_{x3} - m_2\ddot{X}_{G2} = 0 \quad (19)$$

For a rigid couple between tractor and semitrailer (king-pin and fifth wheel) $\ddot{X}_{G1} \cong \ddot{X}_{G2}$ results, approximately, the same longitudinal movement and acceleration, giving:

$$\left(P - F_{x1} - F_{x2}\right)m_2 = \left(-P - F_{x3}\right)m_1 \text{ or } P = \frac{\left(F_{x1} + F_{x2}\right)m_2 - F_{x3}\,m_1}{(m_1 + m_2)} \quad (20)$$

The compressive force P is associated with any unbalanced retarding force between tractor and trailer. To characterise this unbalance, a brake-ratio (br) between tractor and trailer braking forces is defined as:

$$br = \frac{F_{x1} + F_{x2}}{\left(F_{x1} + F_{x2} + F_{x3}\right)} = \frac{F_{tractor}}{F_{total}} \quad (21)$$

This means that for $br = 1$ only the tractor braking forces ($F_{x1} + F_{x2}$) are active. If $br = 0.5$, the trailer braking force (F_{x3}) is 50% of the total braking force applied.

From equations (20) and (21), and after some manipulations, and by using the P_{critic} expression (equation (18)) it is possible to obtain the following expressions:

$$P = a_x\left[\left(1 - br\right)m_1 - br\,m_2\right] \text{ and } a_{x-critic} = \frac{\left(C_{y2}L_2 - C_{y1}L_1\right)}{L_3\left[\left(1 - br\right)m_1 - br\,m_2\right]} \quad (22)$$

where the last expression is the truck critical longitudinal deceleration.

Although this expression is a closed form solution for the critical longitudinal deceleration, factors such as braking distribution, vehicle load transfer during braking and tyre stiffness, all have influence on the terms that appear in equation (22). These will be considered next.

3.1 Braking force distribution

The braking force distribution between tractor and semitrailer should be designed to sustain the best braking proportion. Ideally, the braking of long lorries should be distributed proportionally to the mass of each vehicle.

There are three contributory retarding forces from the braking system for long trucks: the front steering axle brakes (usually hydraulic), the drive axle brakes or motor retarder, and the semitrailer axle brakes (usually pneumatic).

As the real vertical load and dynamic oscillations of the vehicles are not explicitly known, to properly control the braking distribution is not a simple task. The loading sensing valve (*LSV*) installed on the truck suspension is used to measure the load and to control the braking intensity in each axle. The control of the braking distribution is usually performed with a flow-restrictive valve (not a pressure regulator) with an electric/electronic device. Therefore, an unbalanced braking distribution is prone to happen. The brake-ratio (*br*) between tractor and the semitrailer braking force, defined earlier (expression 21), gives this distribution, and may be a parameter to be studied. According to Pinxteren (2010), the maximum typical braking deceleration of a laden semitrailer is between 6.7 m/s^2 and 7.4 m/s^2 for an unladen tractor/semitrailer configuration.

3.2 Tyre stiffness

The tyre properties depend on: the carcass structural properties, inflating pressure and load conditions. The main tyre structural property considered in this approach is the lateral tyre stiffness. The actual tyre load also significantly influences the lateral tyre stiffness. Therefore, the tyre cornering stiffness dependency on vertical load should be taken into account. The relation between the tyre cornering stiffness and the vertical load was found to be almost linear for vertical forces under 40 kN for truck tyres (Luijten, 2010). Therefore, from Figure 5 the ratio of the tyre cornering stiffness to the vertical load for truck tyres is $C / F_z = 5.73[\text{rad}^{-1}]$ (Luijten, 2010). This effect was introduced into the proposed analytical expression.

3.3 Vehicle load transfer

The vehicle dimensions influence the maximum safe deceleration. The vehicle vertical tyre force distribution due to the load is also affected by intensity of the deceleration. As shown in Figure 6, the distance between axles (L_n) and the height of the centre of mass (h_{Gm}, indeed affect the force distribution.

Figure 5 Cornering stiffness of a single truck tyre as function of vertical load (Font: *liujten*)

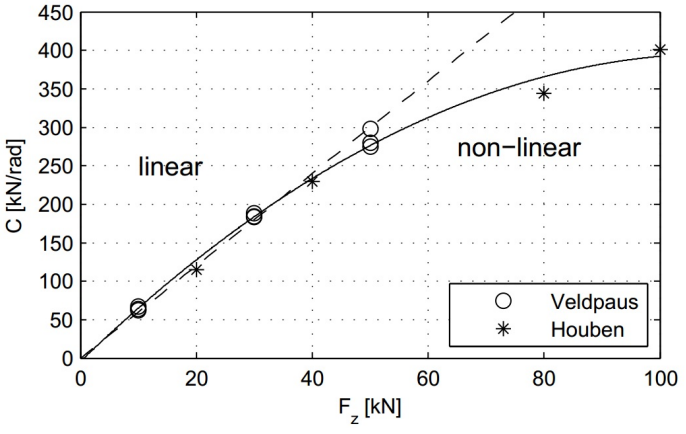

Figure 6 Truck dimensions and the identification of the active forces

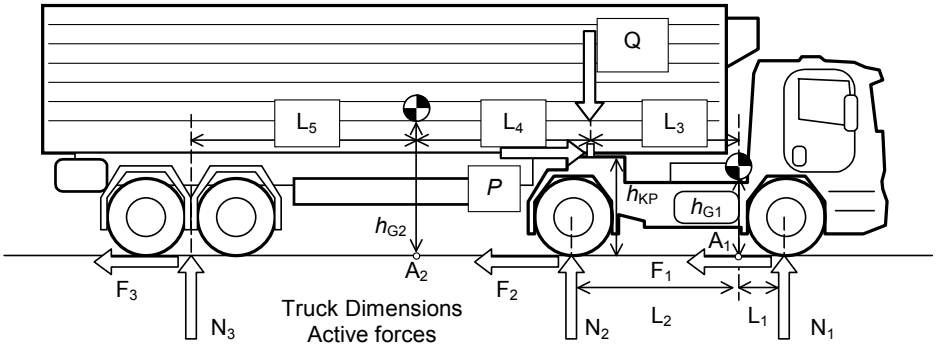

To take into account the truck dimensions, the equations for the translational vertical equilibrium are used for a null vertical acceleration, resulting, for each body (tractor and semitrailer), in the following expressions:

$$N_1 + N_2 = m_1 g + Q \text{ , for the tractor, and } N_3 + Q = m_2 g \text{ , for the semitrailer} \tag{23}$$

The equations for the angular equilibrium for a null angular acceleration affected by a longitudinal acceleration a_x, should also be considered. Taking the pole A_1, on the tractor and the pole A_2 for the semitrailer gives:

$$\sum M_{A_1}^{ext} = N_1 L_1 - N_2 L_2 - m_1 a_x h_{G1} - P h_{KP} + Q L_3 = 0 \tag{24}$$

$$\sum M_{A_2}^{ext} = -N_3 L_5 - m_2 a_x h_{G_2} - P h_{KP} - Q L_4 = 0 \tag{25}$$

The solution of this system of equations (Sanchez, 2017) gives:

$$N_1 = \left(\frac{1}{L_1 + L_2}\right)\left[m_1\left(gL_2 - a_x h_{G1}\right) + P h_{KP} + \left(\frac{L_2 - L_3}{L_4}\right)\left(\left(\frac{m_2 g L_4 + m_2 a_x h_{G2} + P h_{KP}}{L_4 + L_5}\right) L_5 - m_2 a_x h_{G2} - P h_{KP}\right)\right] \tag{26}$$

$$N_2 = \left(\frac{1}{L_1 + L_2}\right)\left[m_1\left(gL_1 + a_x h_{G1}\right) - Ph_{KP} + \left(\frac{L_1 - L_3}{L_4}\right)\left(\left(\frac{m_2 gL_4 + m_2 a_x h_{G2} + Ph_{KP}}{L_4 + L_5}\right)L_5 - m_2 a_x h_{G2} - Ph_{KP}\right)\right] \tag{27}$$

$$N_3 = \frac{m_2 gL_4 + m_2 a_x h_{G2} + Ph_{KP}}{L_4 + L_5} \tag{28}$$

3.4 Expression for the maximum safety deceleration

Considering the planar model, complemented by the braking distribution (equation (21)) and the tyre stiffness, affected by the normal load (equation (27)), it is possible to obtain a simple expression for the maximum safety deceleration (a_{critic}) prior to the yaw instability for the vehicles as:

$$a_{critic} = \frac{\left(C_{y2}L_2 - C_{y1}L_1\right)}{L_3\left[\left(1 - br\right)m_1 - br\, m_2\right]} \tag{29}$$

The lateral tyre stiffness (C_{yi}), which depends on the normal tyre load (according to graph in Figure 5) affected by the load transfer coupled with the acceleration itself (equations (27)), was solved by a *Levenberg-Marquardt* search numeric method.

Using typical truck parameters, as shown in Table 1, one can obtain the maximum safety deceleration values as shown in Figure 7, using the analytic expression given by equation (29).

Figure 7 Maximum safety deceleration as a function of the brake-ratio

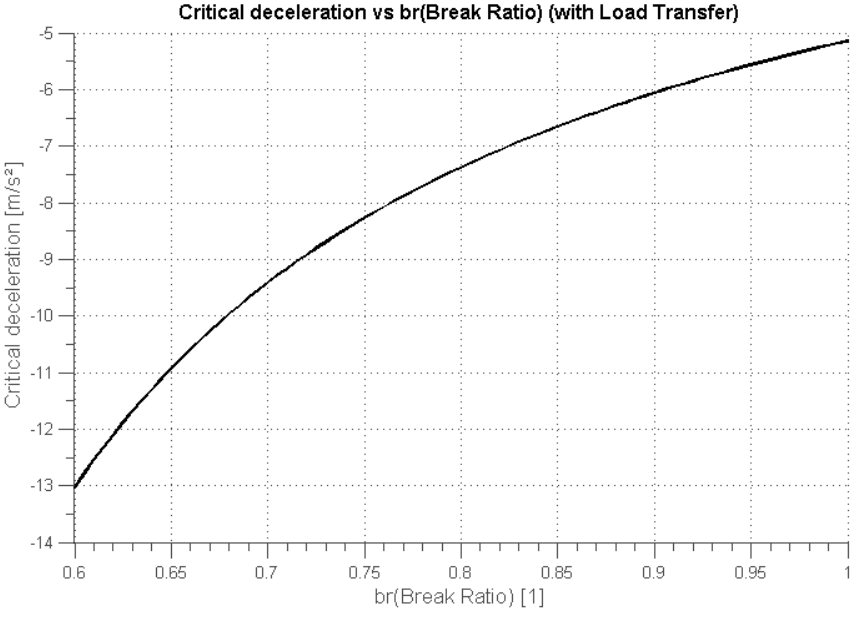

One interesting aspect of this new method is that the maximum safety deceleration expression is not dependent on the speed as the traditional approaches are. By adopting only a simple buckling model, one can predict safety conditions for truck manoeuvres without complex stability analysis or time consuming simulations results (see Figure 9).

Figure 8 Vehicle's position and angular movements

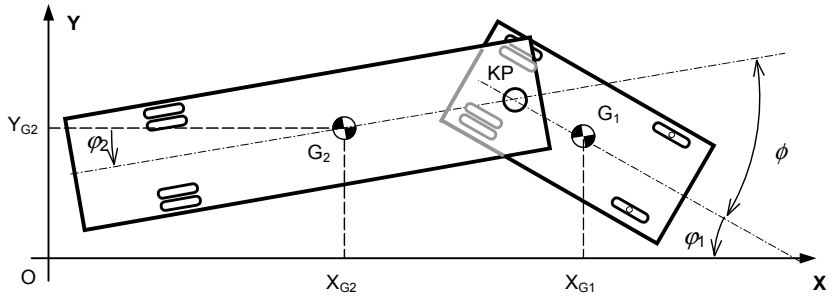

Figure 9 Multibody model (Adams) (see online version for colours)

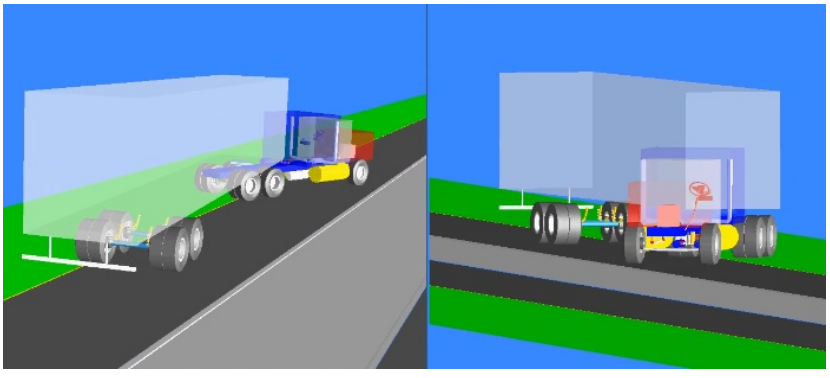

4 Dynamic model of the vehicle

To verify the reliability of the proposed analytical expression depicted in equation 29, for the calculation of the deceleration limit prior to the jackknifing effect, a complete dynamic model of the vehicle, within the same conditions and parameters, was used for validation purposes. A complete non-linear numeric model of the vehicles is used to simulate the stability phenomena. The initial conditions are established (positions, angles and velocities) for a vehicle on a flat and plane surface with fixed and constant friction coefficient of the interaction between tyre and surface. For each brake ratio (br variation), several simulations were performed with the total brake (sum of the brake of the truck and the semitrailer) intensity increased gradually, until the instability occurs (see Figure 10). For each brake ratio value, the correspondent maximum deceleration is identified and stored for comparison purpose. The results of equation (29), for the same conditions and parameters, were then directly compared with the results of the simulation (see Figure 13). The model was developed by Sanchez (2017), and has 19 degrees of freedom and has a similar content to the analytical expression. A two-body articulated

planar motion, shown in Figure 8, and the vehicle's pitch vertical load transfer, due to longitudinal accelerations, are included (Figure 6). The total braking force can be controlled in intensity and distribution between tractor and semitrailer (equivalent to the brake ratio index – br, in equation (19)) to produce asymmetry, generating kingpin force variations. The tyre contact model adopted is linearised to be compatible with the analytical expression, but the inclination at the root is determined by the tyre stiffness properties only. The road surface is flat and clean with a homogeneous friction coefficient. This model is used to simulate the vehicle braking process using a numerical integration algorithm.

Table 1 Typical truck parameters

Parameter	*Value*
Gravity acceleration (g)	9.8 m/s^2
Tractor mass (m1)	7449 kg (A)
Semitrailer mass (m2)	32,551 kg (A)
Normalised lateral stiffness (f_{lat})	5.73 1/rad (A)
Normalised longitudinal stiffness (flong)	0.15 1/rad (B)
Distance between front axle and truck centre of mass – L1	1.1 m (A)
Distance between rear axle and truck centre of mass – L2	2.49 m (A)
Distance between fifth wheel and truck centre of mass – L3	2.49 m (A)
Distance between kingpin and truck centre of mass – L4	4.98 m (A)
Distance between semitrailer rear axle semitrailer centre of mass – L5	3.15 m (A)
Height of truck centre of mass – hg1	1.4 m (A)
Height of semitrailer centre of mass – hg2	2.435 m (B)
Height of kingpin and fifth wheel coupling – hkp	1.4 m (A)
Truck vertical moment of inertia – Jz1	26.608 kg×m^2 (A)
Truck vertical moment of inertia – Jz2	533.917 kg×m^2 (A)

(A) Luijten (2010) and (B) Dunn and Hoover (2004)

4.1 Simulation results and analysis

For comparison purposes, a sudden severe brake action was applied only on the tractor (brake ratio – br = 1.0). The stability of the vehicle was observed via the deceleration intensity (Figure 10(B)), the kingpin force (Figure 10) and the relative angular movement between the vehicles (Figure 11). Beginning at the initial speed of 120 km/h (Figure 10(A)), after one second, the brake is suddenly applied, resulting in an almost constant deceleration (–5 m/s^2 at 1.5 s as shown at Figure 10(B)). The vehicle initially travels straight (Figure 12), on a plane track and no steering counter-action is applied ($\delta = 0$). A quasi-steady-state compression force between vehicles is developed (P force through kingpin, shown at Figure 10(C)).

The vehicles angular behaviour can be analysed from the relative angle (Figure 11(A)) and relative angular speed (Figure 11(B)). The tractor front and rear axle normal forces are also presented (Figure 11(C)).

Figure 10 Results of the simulation for br = 1 (A – speed, B – longitudinal truck deceleration, C – truck/semitrailer coupling force)

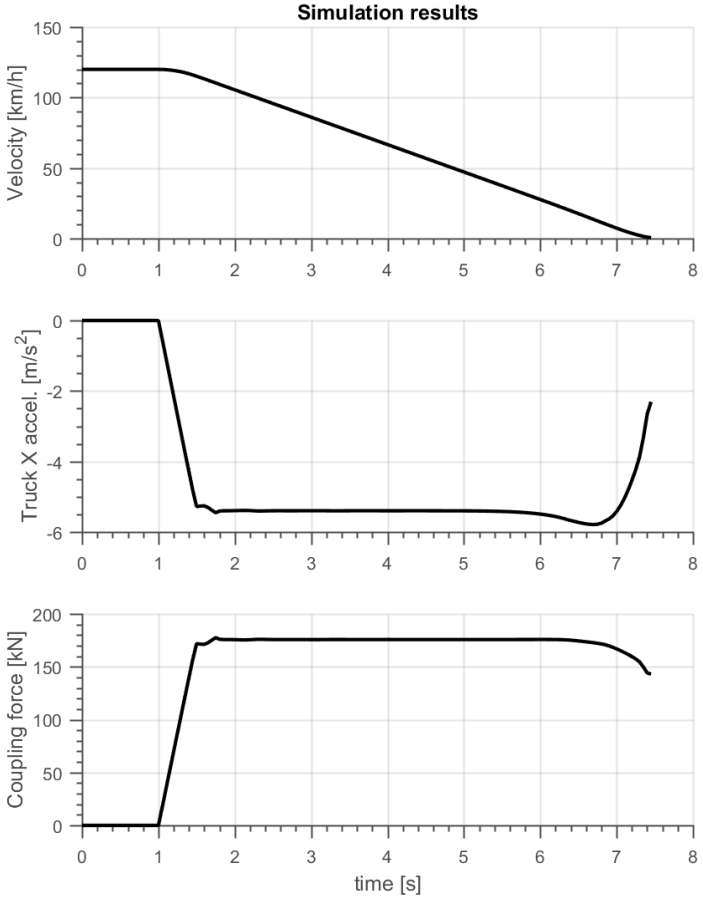

After losing the alignment (jackknifing movement), when the relative yaw angle between vehicles increases drastically (after approximately 5 s – Figure 11(A)), the posterior nonlinear dynamics takes place, with the bodies interacting with each other, trying to recover the controllability, when the set stops (around 7.4 s).

Figure 12 illustrates this movement in sequential time frames, where the jackknifing effect is observed. It is shows the top view of the vehicle trajectory on the xy plane. The red dots are coincident with the location of the vehicle's centre of masses. In this simulation, the brake application is only on the truck (br = 1.0, according to equation 21). It can be seen that the jackknifing movement starts around a 50 m trajectory, and after 5 s of simulation. Vehicle parameters used in the simulation are those presented in Table 1.

It can be seen in Figure 13 that, as the total braking force is increased, the more intense is the deceleration. It also shows that as the more the braking force concentrates on the truck, in detriment of the semitrailer, the greater is the kingpin force. After several simulations with different decelerations levels (total braking force) and braking distribution (truck × semitrailer) the points (*) shown in Figure 13, were obtained.

Figure 11 Results of the simulation for br = 1 (A – relative yaw angle, B – relative angular speed, C – truck axle normal force)

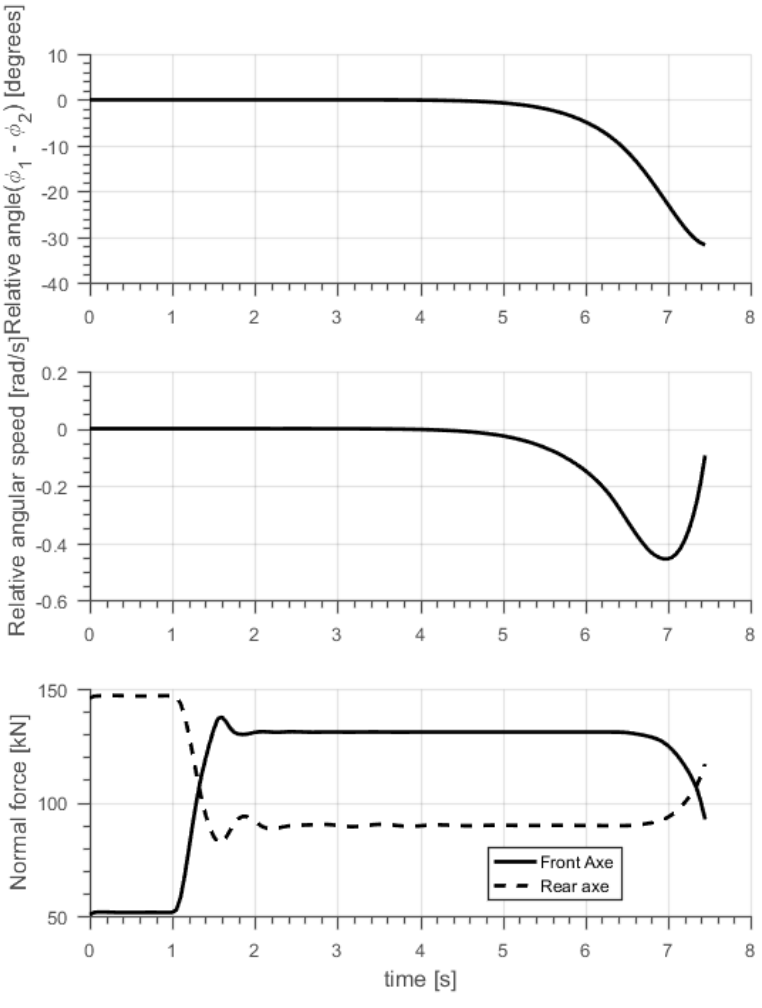

Figure 12 Truck semitrailer trajectory (in metres) (see online version for colours)

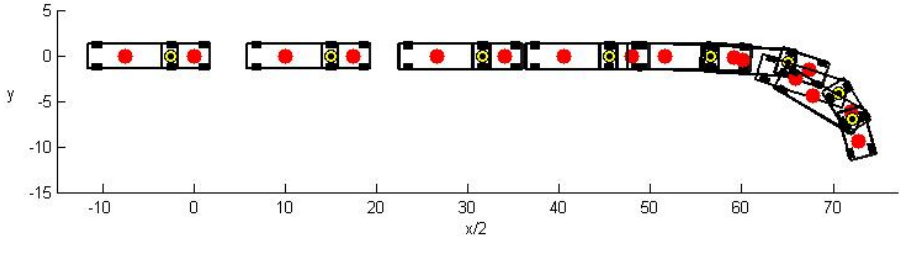

Figure 13 Critical deceleration for different brake ratios (simulation results – marker * and analytical results – solid line)

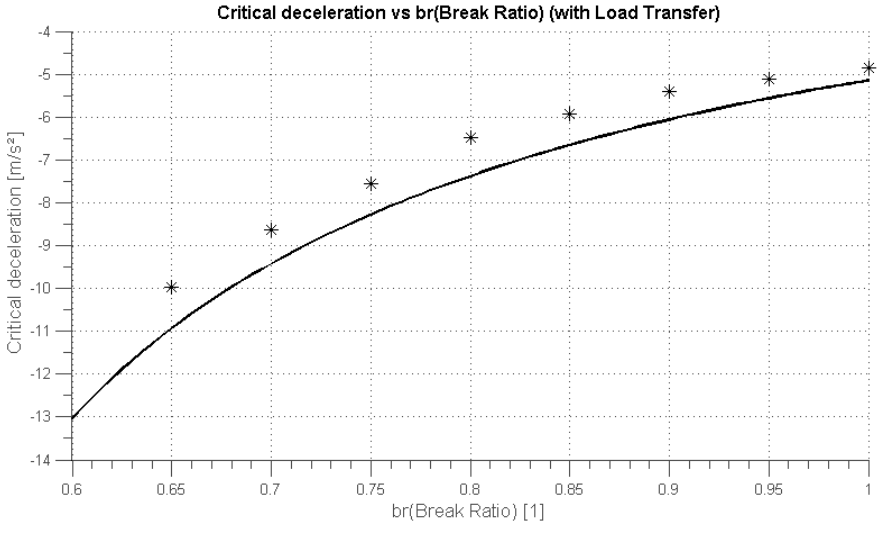

Several simulations with the non-linear model, with different decelerations levels (total braking force) and braking distribution (truck × semitrailer) were performed and plotted in Figure 13 with marker (*). In this figure a comparison of the linear analytical expression (equation (29)) vs. simulated results of the critical acceleration (marker *) as a function of the brake-ratio (br) is presented. It can be seen that the simulation results show good agreement with predictions from the analytical expression. Although the simulations results for critical deceleration are slightly smaller than the results from the linear analytical expression, the same trend is, nonetheless, confirmed.

The analytic expression (equation (29)) reveals the relevant parameters to identify the maximum deceleration limit, prior to the jackknifing effect. The expression is directly related to the vehicle mass distribution (m_1 and m_2), the tyre lateral stiffness (coefficients C_{y1} and C_{y2}) and the vehicle dimensions (distance of each axle to the truck centre of mass L_1 and L_2). It is also an inverse function of the brake ratio (br) as defined on equation (21) (term on the denominator of equation (29)). Additionally, as can be observed in equation (27), the height of the centre of mass of each vehicle (h_{G1} and h_{G2}) does affect the vertical tyre load.

To evaluate the contribution of the variation of the vehicles masses on the maximum safety deceleration, the analytical expression (equation (29)) is used to obtain the results presented in Figure 14, due to the variation of the nominal truck mass (m_1 = 7449 kg) and semitrailer mass (m_2 = 32551 kg).

It can be observed that decreasing the mass of the semitrailer (m_2) the safety limit deceleration is reduced gradually. For example, reducing the semitrailer mass to 60% of its nominal value (see Table 1), the maximum deceleration decreased to –4.6 m/s^2. The opposite merit can be observed for the truck mass (m_1). Therefore increasing the truck mass the safety limit reduces. This analysis can be performed for all the influencing parameters, disclosed in the analytic expression (equation (29)).

Figure 14 Maximum deceleration limit for vehicles mass variations (br = 1)

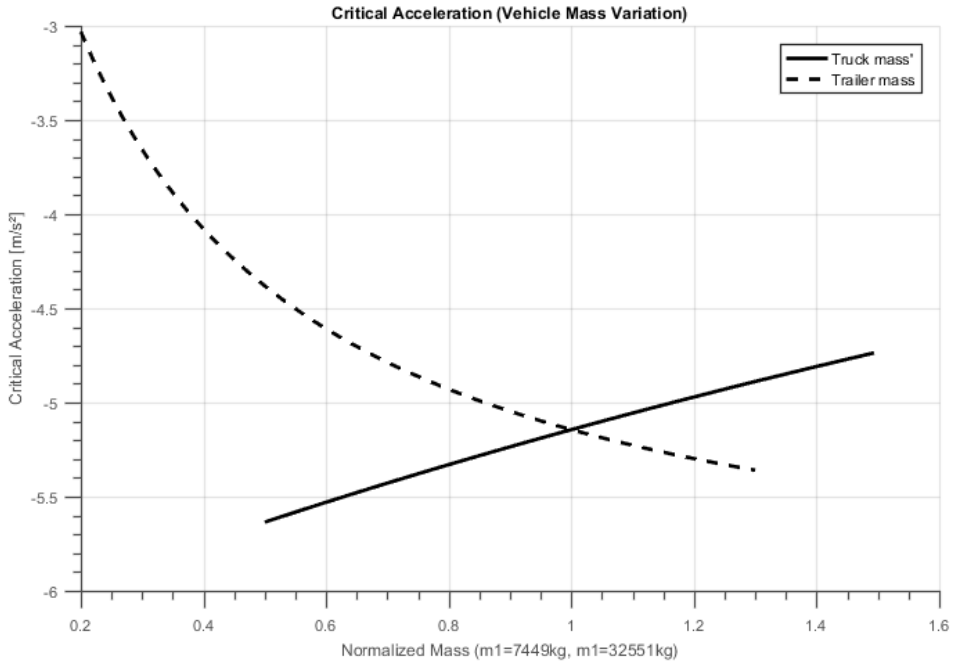

5 Conclusions

A new model based on two articulated bodies with internal inertial force is proposed to describe the yaw angular movement between truck and semitrailer known as jackknifing. An analytical expression is derived, allowing predictions of deceleration limits prior to the yaw instability phenomenon. The distribution of the braking force between truck and semitrailer was considered. The load transfer between semitrailer and truck plays an important role and it is included in the formulation. The tyre stiffness variation due to the vertical load is also included.

As can be observed from the analytic expression (equation (29)), the relevant parameters to identify the maximum deceleration limit, prior to the jackknifing effect, are directly related to the vehicle mass distribution (m_1 and m_2), the tyre lateral stiffness (coefficients C_{y1} and C_{y2}) and the vehicle dimensions (distance of each axle to the truck centre of mass L_1 and L_2). It is also an inverse function of the brake ratio (br). Additionally the height of the centre of mass of each vehicle (h_{G1} and h_{G2}) does affect the vertical tyre load. Therefore, the trend of each relevant parameter can be evaluated individually, as presented in Figures 7 and 14. It should be emphasised that the proposed analytic expression is independent of the vehicle speed and does not require an integration process, unlike all other techniques available in the literature. Therefore it is a new contribution.

The proposed analytical expression was used to calculate the yaw instability limit, related to a deceleration level with a specific braking distribution. The proposed expression is independent of the vehicle speed, and depending only on the vehicle's

internal inertial forces, due to an eventual brake malfunction. A detailed non-linear model with 19 degrees of freedom (item 5) was developed and used as a simulations tool to verify dynamic performance. The results obtained were presented as graphs of the variables in function of the time (truck velocity, longitudinal acceleration, longitudinal inter-vehicle coupling force, relative yaw angle, relative angular speed, the normal forces in each axle). Additionally the truck and semitrailer trajectory was illustrated along the plane showing the yaw angle of the vehicles.

The results were validated by comparison with a complete system dynamic model. Simulations of a braking process on a flat road were performed with the same vehicle's parameters. Braking intensity was progressively increased until the yaw instability occurred. The values of the critical maximum deceleration for different braking-ratios show good agreement between the proposed analytical expression and the numerical simulations.

Acknowledgements

The author wishes to thank the Mechanical Engineering Department at the Polytechnic School of the Universidade de São Paulo (EP-USP), for the support to this research and especially Matheus Lucci Sanchez for the valuable contribution to the model and simulations.

References

Barbosa, R.S. and Costa Neto, A. (1996) 'Dinâmica do Rodeiro Ferroviário – Railway Wheelset Dynamics', *Revista Brasileira de Ciências Mecânicas – ABCM*, Brazil, Vol. XVIII, No. 4, pp.318–329.

Bouteldja, M. and Cerezo, V. (2011) 'Jackknifing warning for articulated vehicles based on a detection and prediction system', *Conference: 3rd International Conference on Road Safety and Simulation*, At Indianapolis, USA.

Chen, L.K. and Hsu, J.Y. (2008) 'Investigation of jack-knife prevention in an articulated scaled vehicle', *Vehicle System Dynamics*, Vol. 46, Suppl. 1, pp.765–777.

Costa Neto, A. (2016) *Vehicle Dynamics Course. Classroom Notes, Escola de Engenharia de São Carlos*, EESC-USP, Brazil.

Ding, N., Shi, X., Zhang, Y. and Chen, W. (2014) 'Analysis of bifurcation and stability for a tractor semi-semitrailer in planar motion', *Vehicle System Dynamics*, Vol. 52, No. 12, pp.1729–1751.

Dunn, A.L. and Hoover, R.L. (2004) *Class 8 Truck Tractor Braking Performance Improvement Study, Report 1, Straight Line Stopping Performance on a High Coefficient of Friction Surface*, National Highway Traffic Safety Administration – Vehicle Research and Test Center – NHTSA/NVS-312. Report nº DOT HS 809 700.

Elhemly, M.A.E., Fayed, M.A.E. and Elmaihy, A.A.E. (2013) 'Tractor–semitrailer jackknifing elimination using semitrailer differential braking technique', *Int. J. Heavy Vehicle Systems*, Vol. 20, No. 1, pp.19–34.

Genta, G. (2006) *Motor Vehicle Dynamics – Modeling and Simulation*, Ed. World Scientific Publishing, p.524.

Kaneko, T., Kageyama, I. and Tsunashima, H. (2002) 'Braking stability of articulated vehicles on highway', *Vehicle System Dynamics*, Vol. 37, Sup. 1, pp.1–11.

Li, X., Chen, W. and Xu, Q. (2016) A *Novel Dynamic Measurement System for Evaluating the Braking Coordination of Articulated Vehicles*, Hindawi Publishing Corporation Journal of Sensors, DOI: 10.1155/2016/8053704, 10 p.

Luijten, M.F.J. (2010) *Lateral Dynamic Behaviour of Articulated Commercial Vehicles*, Master's Thesis – Eindhoven University of Technology – Department Mechanical Engineering, p.121.

Masory, O. and Grainer, T. (2004) 'A simple model for the determination of jackknifing', *Proceedings of the 17th Florida Conference on Recent Advances in Robotics*, pp.1–8.

Pacejka, H.B. (2006) *Tire and Vehicle Dynamics*, 2nd ed., Butterworth Heimann, p.642.

Pinxteren, M. (2010) *Brake and Roll-Over Performance of Longer Heavier Vehicle Combinations*. Master's Thesis at Eindhoven University of Technology, Department of Mechanical Engineering, p.170.

Sanchez, M.L. (2017) *Modelagem, análise dinâmica e controle em um veículo articulado visando prevenir o efeito canivete*.. Trabalho de Conclusão de Curso – TCC, POLI-USP, Brazil. Available at http://www.usp.br/ldsv/?page_id = 462

Talbott, R.M. (1962) 'Simulation of jackknifing moments', *Journal of the Aerospace Sciences*, Vol. 29, Ed nº: 5, pp.606–607.

Wideberg, J. and Dahlberg, E. (2013) 'Effect of the fifth-wheel placement on the stability of articulated vehicles', *International Journal of Heavy Vehicle Systems*, Vol. 20, Ed. 2, pp.144–156, , DOI: 10.1504/IJHVS.2013.053009.

Yuan, H. and Zhu, H. (2016) 'Anti-jackknife reverse tracking control of articulated vehicles in the presence of actuator saturation', *Vehicle System Dynamics*, Vol. 54, No. 10, pp.1428–1447.

Nomenclature

a_G	Acceleration of the centre of mass of the tractor
a_x	Longitudinal component of the acceleration of the tractor
A	Tractor front wheel touch point
Auv	Auxiliary moving reference frame fixed to the wheel
B	Tractor rear wheel touch point
br	Brake-ratio between tractor and semitrailer braking forces
Ci	Tyre stiffness coefficient of the 'ith' wheel
F_{brake}	Brake force
F_{xi}	Tyre longitudinal braking force of the 'ith' wheel
F_{yi}	Tyre lateral forces of the 'ith' wheel
f_{lat}	Normalised lateral stiffness
flong	Normalised tyre longitudinal stiffness
Gxyz	Moving referential frame fixed to the body
g	Acceleration of gravity
Jzi	Tractor vertical moment of inertia of the 'ith' body
KP	Kingpin of the semitrailer
L_n	Distance between the axles and centre of mass G
h_{Gm}	Height of the body 'm' centre of mass,
V_G	Velocity of the centre of mass of the tractor
m_1	Tractor mass

m_2	Semitrailer mass
M_G	Moment of the external forces related to pole *G*
Ni	Vertical load on the '*i*th' wheel
OXYZ	Fixed referential frame
P_{CR}	Buckling critical load
P	Longitudinal force on the kingpin
Q	Vertical force on the kingpin
α_Z	Yaw angular acceleration
$\delta = \delta_1$	Tractor front wheel steering angle
φ	Vehicle yaw angle
$\varphi_1 = \phi_1$	Tractor yaw angle
$\varphi_2 = \phi_2$	Semitrailer yaw angle
ϕ	Relative yaw angle between tractor and semitrailer
k_φ	Elastic angular spring stiffness
ξ_{iy}	Side-slip of the *i*th wheel
C_{iy}	Lateral corner stiffness of the *i*th wheel
V_{iv}	Side-speed of the *i*th wheel contact path
$\vec{V}$	Vehicle velocity
$\vec{i}\ \vec{j}\ \vec{k}$	Tri-orthogonal unit vectors of the moving reference frame fixed to the body
$\vec{u}\,\vec{v}$	Orthogonal unit vectors at point *A* of the auxiliary moving reference frame
$[I]_G$	Tractor inertia matrix, referred to pole G
$[\omega]$	Angular speed vector
$[\dot{\omega}]$	Angular acceleration vector

Appendix A: Dynamic equations

The differential vehicle's equations of motion, based on Sanchez (2017) and Luijten approach (2010), are obtained with the *Lagrange* method. The *Lagrange* equation is stated as:

$$\frac{d}{dt}\frac{\partial L}{\partial \dot{q}_i} + \frac{\partial L}{\partial q_i} = Q_i \text{ where } L = T - U \text{ for } i = 1...n .$$

The geometric dimensions are described in Figures 4 and 6, where $x = x_1 = x_2$ and $y_2 = y_1 - L_3\phi_1 - L_4\phi_2$ and $L_6 = L_4 + L_5$. The generalised coordinates are: $q = \begin{bmatrix} x & y & \phi_1 & \phi_2 \end{bmatrix}^T$

The kinetic energy is: $T = \frac{1}{2}m_1\left(\dot{x}^2 + \dot{y}_1^2\right) + \frac{1}{2}m_2\left(\dot{x}^2 + \dot{y}_2^2\right) + \frac{1}{2}J_{Z1}\dot{\phi}_1^2 + \frac{1}{2}J_{Z2}\dot{\phi}_2^2$

$$T = \frac{1}{2}\left(m_1 + m_2\right)\left(\dot{x}^2 + \dot{y}_1^2\right) + \frac{1}{2}m_2\left(L_3^2\dot{\phi}_1^2 - 2L_3\dot{y}_1\dot{\phi}_1\right) + \frac{1}{2}m_2\left(L_4^2\dot{\phi}_2^2 - 2\dot{y}_1L_4\dot{\phi}_2 + 2L_3L_4\dot{\phi}_1\dot{\phi}_2\right) + \frac{1}{2}J_{Z1}\dot{\phi}_1^2 + \frac{1}{2}J_{Z2}\dot{\phi}_2^2$$

Applying the virtual work principle gives the generalised forces as:

$Q_x = -F_{y1}\delta_1 - F_{y3}\varphi$; $Q_y = F_{y1} + F_{y2} + F_{y3}$; $Q_{\phi_1} = L_1F_{y1} - L_2F_{y2} - L_3F_{y3}$ and $Q_{\phi_2} = -L_6F_{y3}$

The global coordinates are expressed according to the vehicle local coordinates are:

$\dot{x} = u - V_1\phi_1$; $\dot{y}_1 = V_1 - u\phi_1$; $\dot{\phi}_1 = r_1$ and $\varphi = \phi_1 - \phi_2$

The lateral tyre contact forces expressed in the local coordinates are (C_i is the ith tyre stiffness coefficient):

$$F_{y1} = -\frac{1}{u}C_1\left(V_1 + L_1r_1\right) + C_1\delta_1;\ F_{y2} = -\frac{1}{u}C_2\left(V_1 - L_2r_1\right) \text{ and}$$

$$F_{y3} = -\frac{1}{u}C_3\left(V_1 - L_3r_1 - L_6\dot{\theta}\right) + C_3\varphi$$

Taking the following abbreviation between coefficients:

$C = C_1 + C_2$; $C_t = C_3 + C_4$; $C_{s1} = L_1C_1 - L_2C_2$ and $C_{q1}^2 = L_1^2C_1 - L_1^2C_2$

Finally it is obtained the equations expressed in the local coordinates as:

$$\left(m_1 + m_2\right)\left(\dot{V}_1 + ur_1\right) - m_2\left(L_3 + L_4\right)\dot{r}_1 + m_2L_4\ddot{\varphi} = -\frac{1}{u}[\left(C + C_t\right)V_1 + \left\{C_{s1} - C_3\left(L_3 + L_6\right)\right\}r_1$$

$$-C_3L_6\dot{\varphi} - C_tu\varphi + C_1\delta_1 - L_3m_2\left(\dot{V}_1 + ur_1\right) + \left\{J_{Z1} + m_2L_3\left(L_3 + L_4\right)\right\}\dot{r}_1$$

$$m_2L_3L_4\ddot{\varphi} = -\frac{1}{u}[\left(C_{s1} + C_tL_3\right)V_1 + \left\{Cq_1^2 + C_3L_3\left(L_3 + L_6\right) + C_4L_3^2\right\}r_1$$

$$+C_3L_3L_6\dot{\varphi} + C_tL_3u\varphi + C_1L_1\delta_1 - m_2L_4\left(\dot{V}_1 + ur_1\right) + \left\{J_{Z2} + m_2L_4\left(L_3 + L_4\right)\right\}\dot{r}_1$$

$$\left(J_{Z2} + m_2L_4^2\right)\ddot{\varphi} = -\frac{1}{u}\left[-C_3L_6V_1 + C_3L_6\left(L_3 + L_6\right)r_1 + C_3L_6^2\dot{\varphi} - C_3L_6u\varphi\right]$$